Case Study

Assessment of Urban Thermal Environments Using a Combination of the Local Climate Zone and Landscape Ecological Metrics in Taipei City

Yu-Cheng Chen[1]; Tzu-Wen Lo[2]; Wan-Yu Shih[3]; Tzu-Ping Lin[4]; and Kuo-An Hung[5]

Abstract: The urban heat island effect has become a common meteorological phenomenon in urban areas in recent years. Research on urban thermal environments has used various technologies, such as remote sensing, on-site/mobile measurement, and model simulation. This study employed satellite images to comprehensively identify the correlations between thermal environments and the urban morphology in Taipei, Taiwan. This study applied the local climate zone (LCZ) scheme to classify urban land types by surface characteristics. The LCZ classification result was used as the basic unit for assessing and calculating urban forms by the landscape ecological metrics (LEM). For the thermal environment information, this study collected air temperature data by mobile measurements and combined it with records from weather stations. The results showed that different urban form compositions were associated with thermal environments. Built-up areas with higher levels of edge density tended to have higher heat intensity. For two regions with the same proportion of green spaces and built environments, the temperature varies with different configurations. This study can evaluate the urban thermal environments and assist urban planners who do not have a meteorological background in finding urban climate issues and developing heat mitigation strategies.
DOI: 10.1061/JUPDDM.UPENG-4890. © *2024 American Society of Civil Engineers*.

Author keywords: Air temperature; Landscape ecology metrics; Local climate zone; Urban thermal environment; Urban heat island.

Downloaded from ascelibrary.org by Kuo An Hung on 02/28/24. Copyright ASCE. For personal use only; all rights reserved.

Introduction

In Taipei, Taiwan, more than 98% of the population lives in an urban planning district (Department of Civil Affairs, Taipei City Government 2022); building volume is increasing, while the total area of green spaces is decreasing; the urban thermal stress has thus become a major threat to sustainable urban development (Ren et al. 2013; Chen et al. 2017; Lin et al. 2017; Chen et al. 2019a).

In addition, warmer conditions are already causing several issues around the world, including public health, where previous studies have shown that an increase in the frequency and severity of heat waves can lead to an increase in illness and death, especially among young children, the elderly, and the poor (Kovats and Hajat 2008; Campbell et al. 2018; Dong et al. 2020; Ebi et al. 2021; Arsad et al. 2022). As global temperatures rise, crops are wilting due to high temperatures, and agricultural yields in more countries are beginning to be affected (Zhao et al. 2017; Becker et al. 2023; Hung et al. 2023). Even in terms of public safety, high temperatures can cause people to become more agitated and stressed, which can lead to an increase in violent crime (Tiihonen et al. 2017; Harp and Karnauskas 2020), and it is also worth recognizing that as global warming progresses, the proportion of natural disasters, such as extreme flooding, will also increase significantly (Schiermeier 2011; Tabari 2020; Gu et al. 2022; Alifu et al. 2022). Therefore, understanding the relationship between urban landforms and the urban climate and developing a strategy to mitigate adverse thermal environments are essential.

In urban areas, the urban heat island (UHI) has been a significant climate phenomenon in recent years, and numerous cities including St. Lawrence in Canada (Oke 1973), Phoenix in the United States (Baker et al. 2002), Nagpur in India (Kotharkar and Surawar 2016), and Tainan (Chen et al. 2018) and Taipei (Chen et al. 2019b) in Taiwan are suffering from heat stress due to intensive development. Many countries, including Hong Kong (Jia and Wang 2021), Taiwan (Lin et al. 2017), Singapore (Teo et al. 2022), China (Qin et al. 2023), and Australia (Heshmat Mohajer et al. 2022), are developing approaches for identifying hotspots to slow down the increase and mitigate thermal loads. Based on local knowledge of urban climate conditions, governments and urban planners can identify areas with the highest thermal stress and adopt regulations to mitigate the thermal load through urban planning and building renovation.

Studies evaluating urban climates have used various urban parameters such as population density, total building area, surface impermeability, land use, land cover, and geographical features and have proven that urban landforms contribute to variations in urban climate (Oke 1988; Honjo et al. 2015; Wei et al. 2016; Zhou et al. 2017; Shih 2017; Zhang et al. 2017; Giridharan and Emmanuel 2018). However, if the study only focuses on intuitive factors, such as the percentage of area and density in the region, but ignores the state of urban form composition, such as the distribution features and the level of connectivity with the surrounding

[1]Dept. of Architecture, Nanhua Univ., No. 55, Sec. 1, Nanhua Rd., Dalin Township, Chiayi 622, Taiwan. ORCID: https://orcid.org/0000-0002-4315-2608. Email: leo2208808@gmail.com

[2]Dept. of Architecture, National Cheng Kung Univ., No. 1, Univ. Rd., East Dist., Tainan 701, Taiwan. Email: s8619731@gmail.com

[3]MS Program in Disaster Risk Reduction and Resilience, International College, National Taiwan Univ., No. 1, Section 4, Roosevelt Rd., Da-an District, Taipei 10617, Taiwan. Email: wyshih@ntu.edu.tw

[4]Dept. of Architecture, National Cheng Kung Univ., No. 1, Univ. Rd., East Dist., Tainan 701, Taiwan. ORCID: https://orcid.org/0000-0003-3961-9858. Email: lin678@gmail.com

[5]Dept. of Architecture, National Cheng Kung Univ., No. 1, Univ. Rd., East Dist., Tainan 701, Taiwan (corresponding author). ORCID: https://orcid.org/0000-0002-1850-0500. Email: hungkuoan@gmail.com

Note. This manuscript was submitted on August 15, 2023; approved on December 12, 2023; published online on February 28, 2024. Discussion period open until July 28, 2024; separate discussions must be submitted for individual papers. This paper is part of the ***Journal of Urban Planning and Development***, © ASCE, ISSN 0733-9488.

area, it will lead to differences in the thermal environments of different morphological features in the same area or density. Therefore, morphological characteristics are included in this study for the association with the thermal environments. In addition, investigation of the cause of thermal stress is complicated for areas with insufficient data. For example, obtaining sufficient information on climate and the urban built environment in every city has been difficult because it has either been lacking or controlled by the government due to security issue or privacy protection issues (Figueiredo and Martina 2016; Oraskari and Törmä 2017; Chen et al. 2019a).

Therefore, this study employed free Landsat-8 satellite images, which are easily downloadable, to obtain information about the built environment and used meteorological information obtained by the Taiwan Central Meteorological Bureau to understand the relationship between urban morphology and climate.

Another issue is that mixed land use in cities makes it difficult to quantify urban patterns and analyze the relationship between thermal environment and land use (Hu and Jia 2010; Su et al. 2010; Kim et al. 2019). Information on land use composition is also not three-dimensional, even though a city's three-dimensionality is a crucial factor affecting the thermal environment (Yahia and Johansson 2014; Yang et al. 2018; Chen et al. 2020; Yang et al. 2020).

Therefore, this study assessed the urban thermal environment in Taipei using two systems: local climate zone (LCZ) classification and landscape ecological metrics (LEM) and developed an approach that can be used to comprehensively evaluate not only land use but also morphology to investigate urban thermal environments. The approach uses accessible satellite images and the LCZ scheme that interprets urban development patterns into three-dimensional information as a foundation to analyze land configuration characteristics using the LEM.

By using the proposed method of first classifying the urban grid into different LCZs and then analyzing the grid distribution pattern of each LCZ through the LEM, it will be possible to more clearly identify the impacts of urban form and the characteristics of their composition on thermal conditions in different regions and recommended building configurations and suitable layouts of green space to reduce the urban thermal load in the future.

Methods

Study Area

Taipei is a big city with compact, developed urban areas. The city is approximately 271.8 km^2 in size (Fig. 1), with a 2.69 million population in 2017 (Department of Civil Affairs, Taipei City Government 2017). Taipei, located in a subtropical monsoon climate, has the highest population density in Taiwan. Because of its topographical characteristics, hot air tended to be trapped in the basin area in summer, resulting in a higher city temperature than the surrounding area. According to meteorological statistics published by the Central Weather Bureau from 1981 to 2010, the average annual temperature is 23°C, with the hottest month being July, which has an average monthly temperature of 29.6°C. The coldest month is January, with an average monthly temperature of 16.1°C (CWBT 2011).

In this study, Taipei was used to investigate the relationship between urban morphology and climate. As Taipei's development intensity is high, it is essential to pay attention to heat mitigation in current warming trends.

Local Climate Zone

The descriptions and definitions of various artificial and natural environments vary by country. Therefore, to establish an urban classification approach that can be adapted by each user, standard climatic and environmental factor guidelines had to be systematically established.

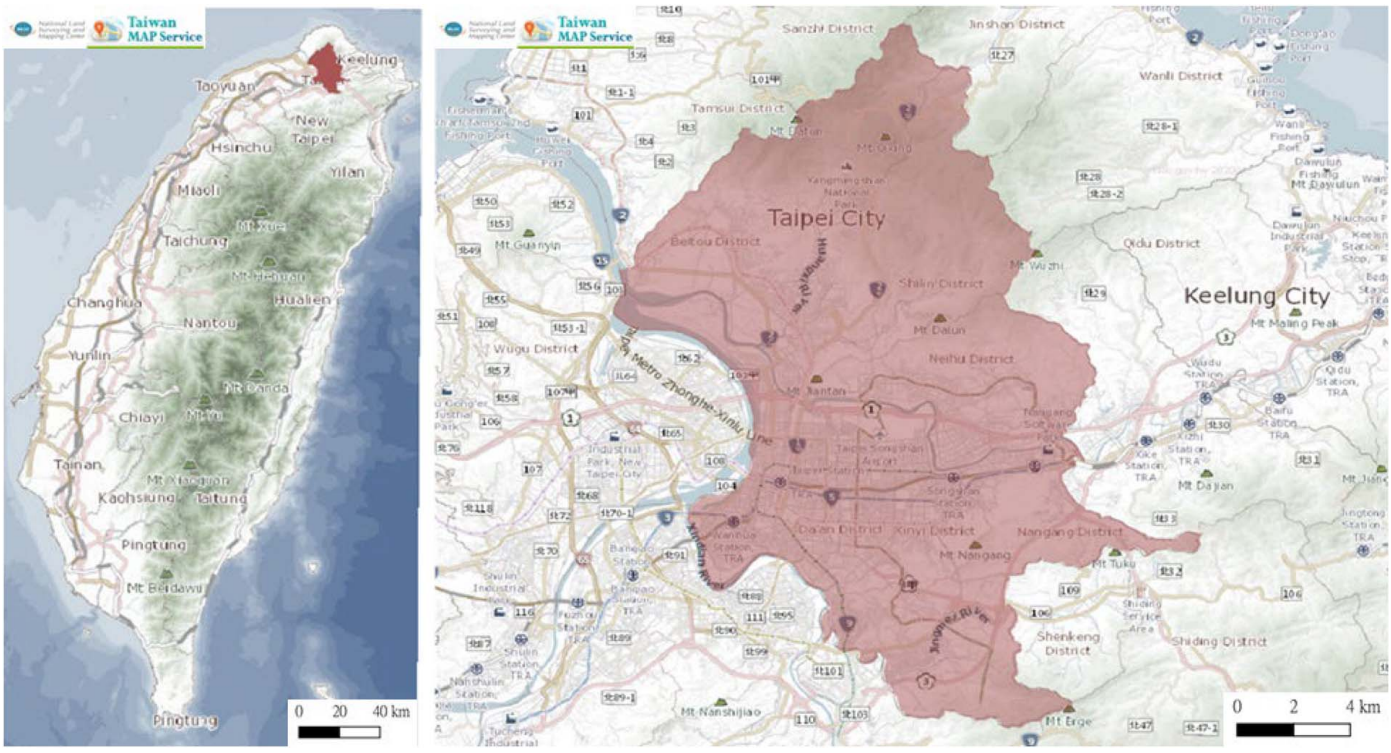

Fig. 1. Location of Taipei. (Map from the National Land Surveying and Mapping Center, Taiwan MAP Service.)

Downloaded from ascelibrary.org by Kuo An Hung on 02/28/24. Copyright ASCE. For personal use only; all rights reserved.

Unlike other classification systems, the scheme mainly uses differences in the built-up environment to sort land in more detail and introduces density, openness, height, category of use, and natural environment density (Stewart and Oke 2012; Stewart et al. 2014). LCZ has often been used in studies to determine the urban environment's impact on thermal environments (Bechtel et al. 2015; Cai et al. 2016; Kaloustian and Bechtel 2016; Beck et al. 2018). In this study, LCZ was used as a primary patch to construct each LEM range and quantify the various LEM indicators.

Local Climate Zone Classification System

Stewart and Oke (2012) proposed the first local climate zone system. They performed a series of quantifications and verifications of related data and information, including sky visibility, building height, street aspect ratio, building projected area, impervious floor area ratio, average building height, and surface roughness. LCZ classification is used to divide the urban pattern into 17 types of areas by using Landsat-8 images. The classification and naming form was LCZx, where x denotes Numbers 1–10 in built-up areas and Letters A to G in nonbuilt-up areas (Stewart and Oke 2012).

In this study, data from the Landsat-8 satellite on July 7, 2017 were used to classify LCZs. The satellite has a resolution of 30 m, carries 11 spectral bands, and passes over the same area every 16 days. The classification results also exclude the error value caused by cloud and fog conditions.

Classification Process

The LCZ classification process was based on the World Urban Database and Access Portal Tools (WUDAPT) project. The entire system uses the satellite image as the basic reference layer and employs Google Earth and the supervised classification method to frame the demonstration area manually. The final classification process was performed and automated using SagaGIS software (vesrion 2.2.0). The resolution of LCZ classification was 100 m × 100 m in this study to prevent a small scale from leading to environmental illusions and a large scale from decision errors (Bechtel et al. 2015).

Combined Use with Landscape Ecology Metrics

This study integrates similar urban patterns to reduce the impact of analysis of classification errors in LEM's subsequent calculation.

The original 17 surface LCZ types were further classified into 7 general surface types according to their characteristics. Building density and building use characteristics were summarized into general categories, including densely built areas, open built areas, lightweight construction areas, suburbs, industrial areas, planting areas, and water bodies (Fig. 2).

Landscape Ecology Metrics

LEM is an algorithm that quantifies specific spatial patterns, characteristics of patches, and classes of patches (Turner et al. 2001; Leitão and Ahern 2002; Uuemaa et al. 2009, 2013); it has been used to explore the relationships between the climate, geography, ecology, economy, society, and culture of the landscape condition (Forman 1995; Syrbe and Walz 2012; Frank et al. 2012; Zhang et al. 2013; Kong et al. 2014).

Landscape ecology argues that landscape structure influences ecological processes (Naveh and Lieberman 1985; Turner 1989; Wu 2000). The LEM was originally designed to quantify the changes in biological habitats and ecological environments. The field of landscape ecology has been increasingly applied to urban areas for describing landscape structure and land-use changes.

In this study, the LEM was used to quantify the characteristics of land patterns and attempted to identify urban structures by using the four LEM indexes—percent landscape (PLAND), large patch density (LPI), edge density (ED), and fractal dimension–area-weighted (FRAC_AM)—to investigate whether an area composed of multiple LCZs has different effects on the urban thermal environment with air temperature (Ta) under differing content structures and patterns.

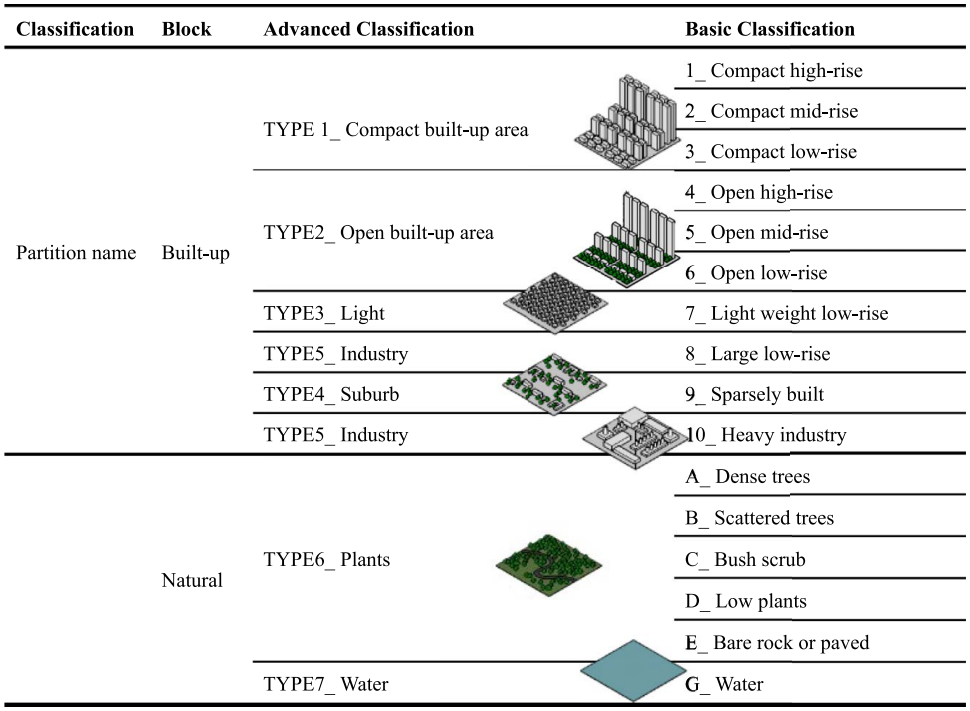

Fig. 2. Comparison between the LCZ basic classification and advanced classification.

Downloaded from ascelibrary.org by Kuo An Hung on 02/28/24. Copyright ASCE. For personal use only; all rights reserved.

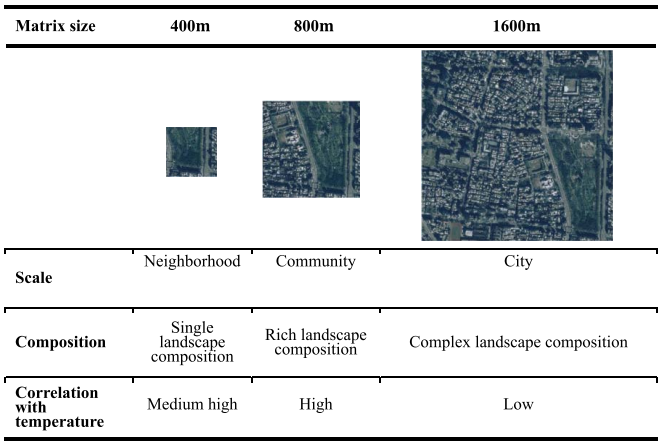

Fig. 3. Landscape grid size specification. (Image courtesy of the USGS, Landsat-8.)

Matrix Size

The matrix size of the landscape is affected by a particular study area. This study aimed to explore differences in urban land types, and the resolution of the landscape unit LCZ was 100 m, which can easily present the morphology feature on an urban scale.

In this study, when defining the size of the landscape matrix and considering the basic unit of an LCZ of 10,000 m^2, the landscape matrix sizes of 160,000 m^2 (400 m × 400 m), 640,000 m^2 (800 m × 800 m), and 2,560,000 m^2 (1,600 m × 1,600 m) were employed in the analysis to confirm the correlation with Ta (Fig. 3). The results revealed that a matrix of 2,560,000 m^2 would lead to the lack of a single type category in calculating the index. The 160,000 m^2 matrix size would be affected by the unit of the LCZ, and LEM calculations would be strongly affected by a single surface type.

Besides, the 400- and 1,600-m landscape ranges were compared with the 800-m landscape range. In the grid, the LEM calculation value of the 800-m landscape range was positively correlated with the temperature and could reflect a more prosperous landscape composition; therefore, the grid size of the landscape range used in this study was 800 m.

Level Description

The spatial structure of the LEM was divided into two levels in this study: the class and patch levels. A landscape matrix was defined as the range 800 m × 800 m, and thus, a landscape contained 64 LCZ units because LCZ with a resolution of 100 m was used as the surface-type unit. The patch level is the minimum level of the LEM and describes each unit's appearance in the landscape (Fig. 4).

The class level was based on the seven major surface types of LCZ after secondary classification, indicating that at least one and up to seven surface types coexist in a landscape. The category hierarchy was used to describe the individual characteristics—PLAND, LPI, ED, and FRAC_AM—of each surface type in a landscape and quantify the surface differences other than differences in area. Therefore, in a landscape, the class level index had a particular value in each class.

Indicator Explanation

The LEM analysis revealed various landscape characteristics according to differences in the spatial scale of the indicators. As described in section "Level Description," this study extracted the class level to analyze urban-scale environmental factors. The analysis of class-level indicators described the spatial distribution of a class in a landscape. Therefore, when calculating the LEM, spatial pattern distribution values were obtained for all landscape types. This study used PLAND, LPI, ED, and FRAC_AM. PLAND and LPI represent the proportion of a type of area in a landscape, whereas ED and FRAC_AM reveal the type of distribution shape in a landscape (Table 1).

PLAND represents the percentage of an area in a landscape and ranges between 0 and 1. LPI represents the block group with the largest area in a landscape and ranges between 0 and 100. ED indicates the degree of contact in a landscape and ranges between 0 and 100. FRAC_AM represents the shape complexity in a landscape and ranges between 1 and 2.

Calculation Tool

This study calculated the LEM using the FRAGSTATS software (version 4.2.1) package (McGarigal and Marks 1995). This software can calculate map files in various ways, and this study used ArcGIS to process the gridded surface classification map files in image batch processing for calculation, generated various LEM distribution maps, and quantified the LEM values in each grid.

Obtaining the Urban Thermal Environment

Meteorological Stations

This study's temperature information was obtained from 14 meteorological stations of the Taiwan Central Meteorological Bureau in Taipei [Fig. 5(a)] in July 2017. The data were then processed through the inverse distance weighted (IDW) interpolation to obtain Taipei's overall air temperature.

Mobile Measurements

In addition to collecting the Ta from weather stations, this study manually performed mobile measurements to verify the Ta and perform related analysis. The measurements were made by a private car equipped with measuring instruments, including a thermometer and global positioning system. The sensor was equipped with a ventilation shield to prevent the sun from shining directly on the sensor to get a good temperature information quality, and adequate ventilation was maintained to achieve a balanced air temperature measurement [Fig. 5(b)].

To reduce errors in the temperature and location measurements caused by the instrument's reaction time, this study controls the car driven during measurement at slower than 20 km/h. The route surrounded the entire developed area of Taipei, but roads were occasionally blocked, and the car could not enter the northern mountainous area. The main route surrounded the city's built-up area.

Results

Initial Mapping Results

LCZ Distribution

The surface LCZ classification of Taipei is displayed in Fig. 6. Throughout Taipei, the LCZs comprised LCZA (dense trees) in the south and north, whereas a developed corridor runs east to west through the city. The major built-up areas were LCZ2 (compact high rises), LCZ6 (open low rises), and LCZ9 (sparse

Downloaded from ascelibrary.org by Kuo An Hung on 02/28/24. Copyright ASCE. For personal use only; all rights reserved.

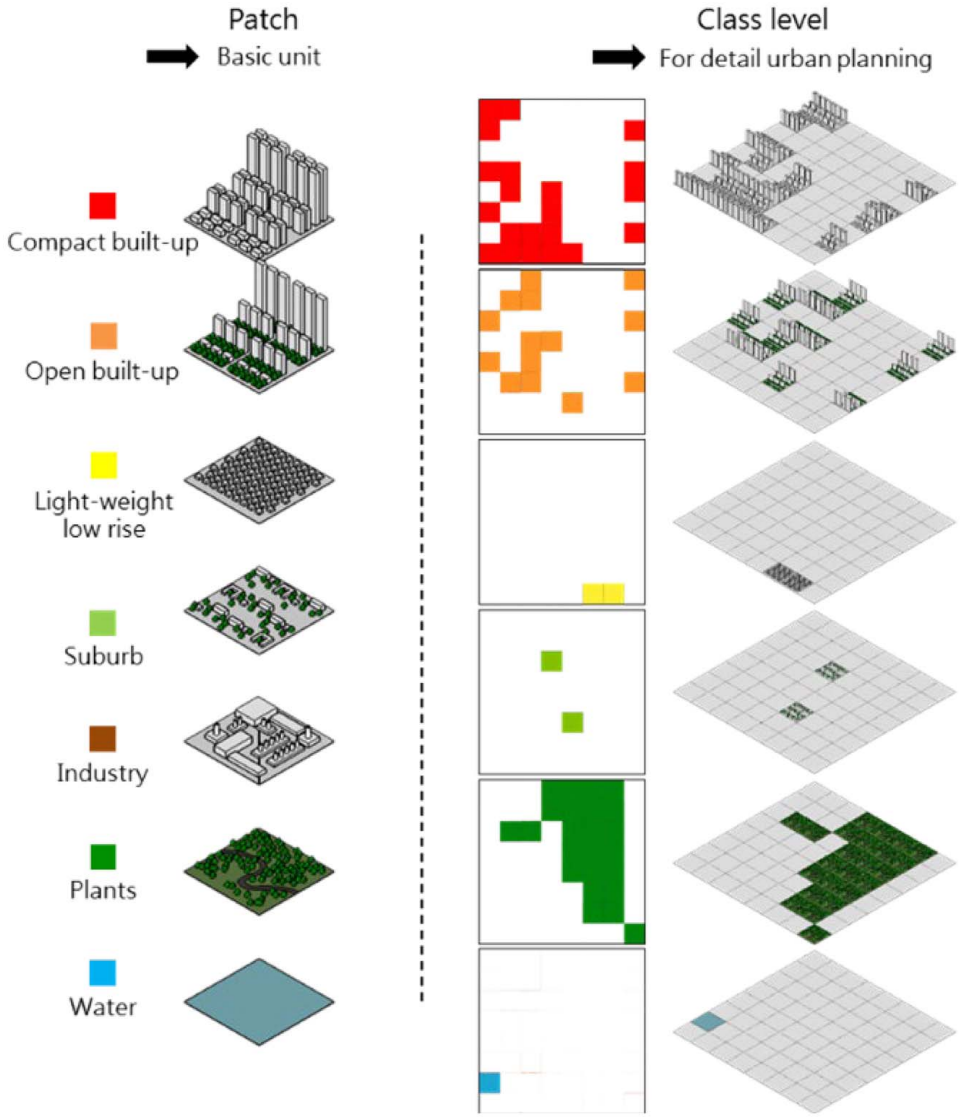

Fig. 4. LEM patch and class level demonstration.

buildings). Most of the LCZs in the nature areas were LCZA (dense trees) or LCZG (water).

The classified images revealed the urban development trend in Taipei. The built-up areas were concentrated in the center and west, whereas the northeast and southeast were mostly mountainous and suburban areas.

The built environment close to the mountainous area was mostly classified as an open built area, and the east–west axial areas in which development has been concentrated were mostly classified as densely built areas. Few large green spaces exist in the city. Other green spaces were mostly scattered in small parks. The water body areas were mainly rivers.

Table 1. Calculation equation of the class-level index

Class level	Index	Meaning
Area	PLAND Percent landscape	Proportion of the patch $= a/A \times 100\%$ a = class area; and A = landscape area
	LPI, large patch density	A measure of the largest patch area of the type $= \dfrac{\text{Max}(a_1, \ldots, a_n)}{A}$ a = class area; and A = landscape area
Shape	ED, edge density	The sum of the length of all patch edges divided by the total area of the landscape $= \sum_{k=1}^{m} e_{ik}/A$ e = class edge length; and A = landscape area
	FRAC_AM, fractal dimension_ area weighted	A measure of departure from Euclidean geometry $E = ka^{Fd/2}$, $F_d = 2\ln\left(\dfrac{P}{k}\right)/\ln(A)$ e = class edge length; and a = Class area, $k = 4$

Downloaded from ascelibrary.org by Kuo An Hung on 02/28/24. Copyright ASCE. For personal use only; all rights reserved.

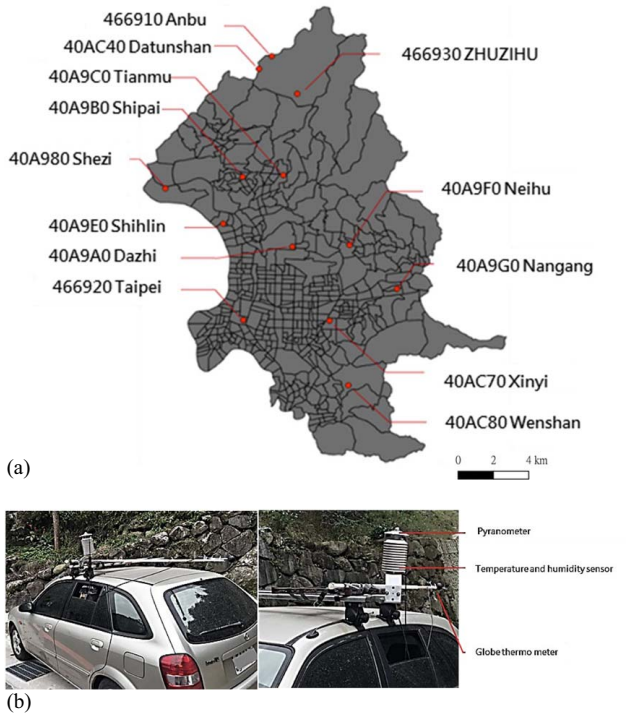

Fig. 5. (a) Location of Taipei Weather Stations; and (b) mobile measurement with equipment.

LEM Composition

This study investigated the impact of the urban built environment on a city's thermal load. Therefore, before the analysis, the standard of the Taipei built environment was first defined.

Seven surface types were identified, five of which were types of built-up environments. Given this and the 800-m landscape grid spatial characteristics, this study defined a built environment as either a landscape containing three or more surface types or a landscape with an area at least 25% of Types 1–5.

The highest area ratios were densely built areas (Type 1) and green belts (Type 6). These two types accounted for most of the environment in Taipei, and the city's climate environment would thus be most strongly affected by these types. Therefore, in the follow-up analysis, this study focused on the compact built-up and plant areas in the built environment using four class-level indicators to describe the relationship between land pattern distribution and Ta (Fig. 7).

Air Temperature Distribution

This study used weather station data and mobile measurements to obtain Ta information. Fig. 8 presents the temperature distribution in Taipei based on the average daytime data from 08:00 to 16:00 in July 2017.

As revealed by the Ta distribution map, Ta ranged from 23.4°C to 35.5°C. The high-temperature trend was closely related to the distribution density of the built environment (Fig. 8). The high-temperature area was concentrated in the center and west of Taipei, whereas the mountainous areas in the north and south had lower temperatures.

The temperature distribution also shows that the air temperature in the densely built environment areas was higher; the temperature was lower only around the riversides and near mountains.

Air Temperature in the LCZs

The Ta distribution in July daytime (08:00–16:00) in each LCZ region (Fig. 9) indicates that LCZ1 had a higher temperature than similarly highly built-up areas because the compact obstacle

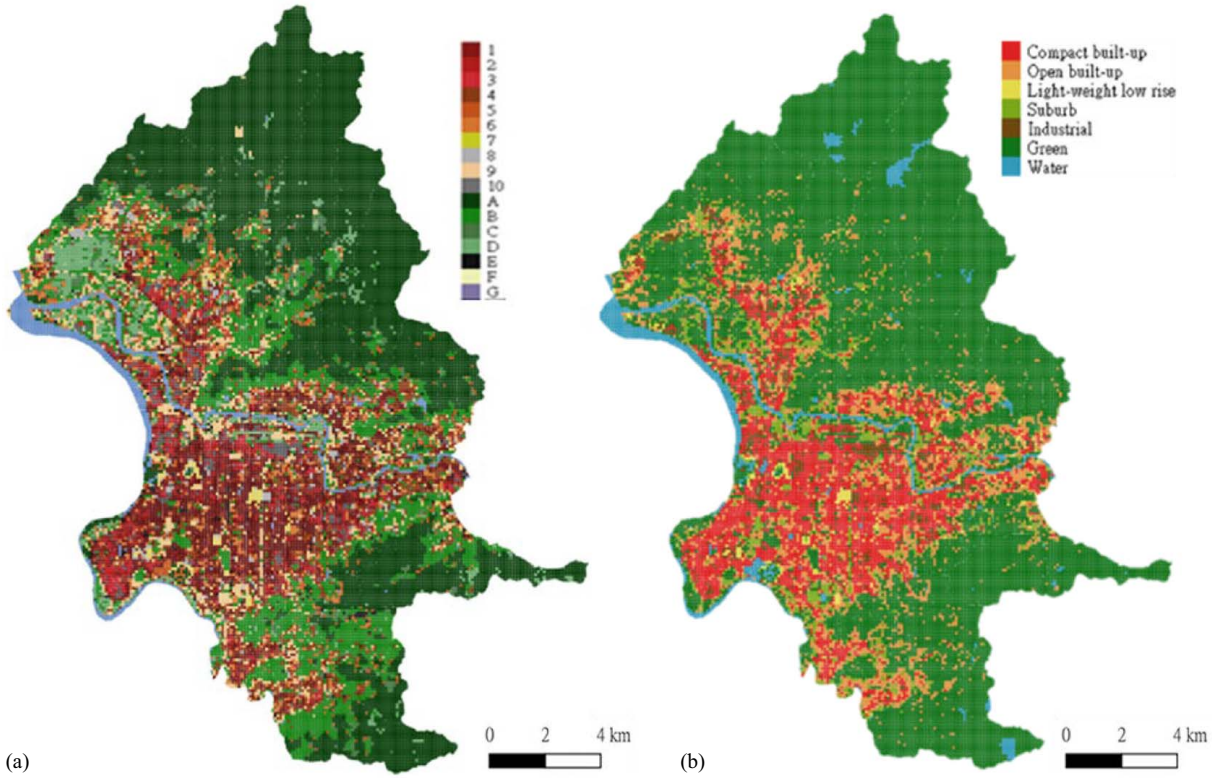

Fig. 6. LCZ classification results in (a) 17 types; and (b) 7 general surface types.

Downloaded from ascelibrary.org by Kuo An Hung on 02/28/24. Copyright ASCE. For personal use only; all rights reserved.

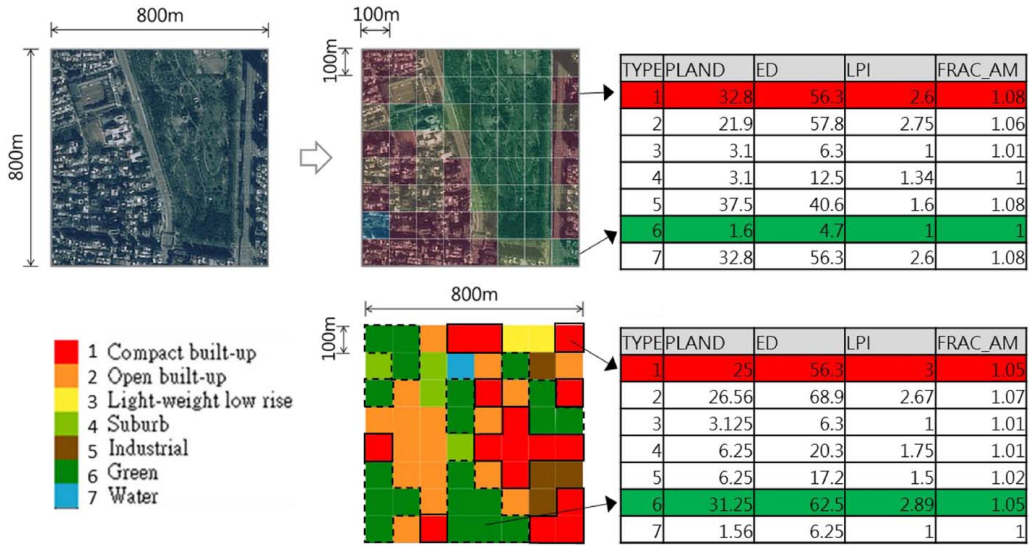

TYPE	PLAND	ED	LPI	FRAC_AM
1	32.8	56.3	2.6	1.08
2	21.9	57.8	2.75	1.06
3	3.1	6.3	1	1.01
4	3.1	12.5	1.34	1
5	37.5	40.6	1.6	1.08
6	1.6	4.7	1	1
7	32.8	56.3	2.6	1.08

TYPE	PLAND	ED	LPI	FRAC_AM
1	25	56.3	3	1.05
2	26.56	68.9	2.67	1.07
3	3.125	6.3	1	1.01
4	6.25	20.3	1.75	1.01
5	6.25	17.2	1.5	1.02
6	31.25	62.5	2.89	1.05
7	1.56	6.25	1	1

Fig. 7. Calculation method of LEMs. (Image courtesy of the USGS, Landsat-8.)

provided by LCZ1 led to poor ventilation and increased anthropogenic heat storage in the area.

The built-up blocks with high temperatures were LCZ1–3, LCZ8, and LCZ10. In addition to the high temperature in LCZ1–3 caused by high building density, LCZ8 and LCZ10 were industrial blocks and hotspots, respectively. Furthermore, plant blocks provided cooling resources.

LCZA had the lowest temperature in the entire class. Other low-temperature areas were LCZB–D, which were natural environments. However, LCZE, classified as artificial pavement, accounted for the highest temperature in the plant block classification because of pavement's low water permeability and high heat storage capacity.

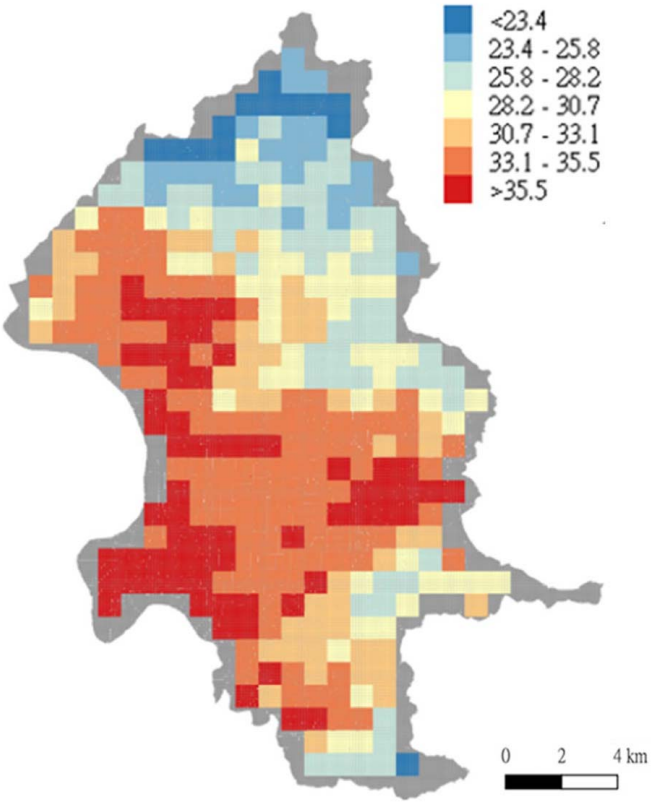

Fig. 8. Air temperature distribution map in Taipei.

Relationship between the Landscape Ecology Index and the Thermal Environment

In this study, summer day Ta was used as the main parameter to represent the urban thermal environment. The major integrated LCZ classifications each represented a type of urban area, and correlation analysis was performed by considering densely built areas and green spaces, which were the most common in the city and would have the most substantial effect on the urban climate. For the quantification of urban types, please refer to the class-level indicators' description in section "LEM Composition." The four selected indicators—PLAND, LPI, ED, and FRAC_AM—were used to evaluate the relationship between landscape ecology index and the thermal environment by simple regression analysis.

Impact of the Built-Up Environment on the Thermal Environment

The relationship between Ta and LEM revealed that densely built areas accounted for approximately 0%–90% of a landscape area, and all four parameters of the densely built areas—the area-related PLAND and LPI and shape-related ED and FRAC_AM—were

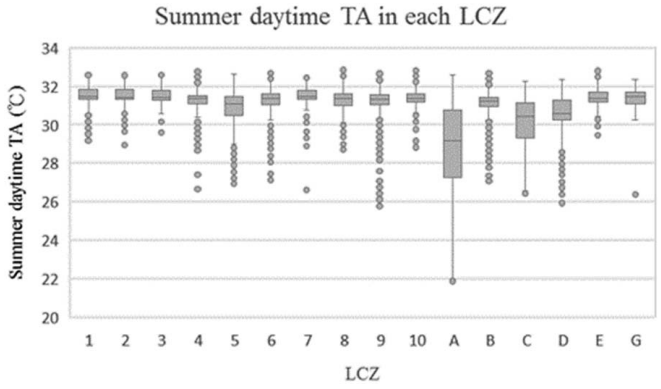

Fig. 9. Distribution of air temperature in different LCZs.

Downloaded from ascelibrary.org by Kuo An Hung on 02/28/24. Copyright ASCE. For personal use only; all rights reserved.

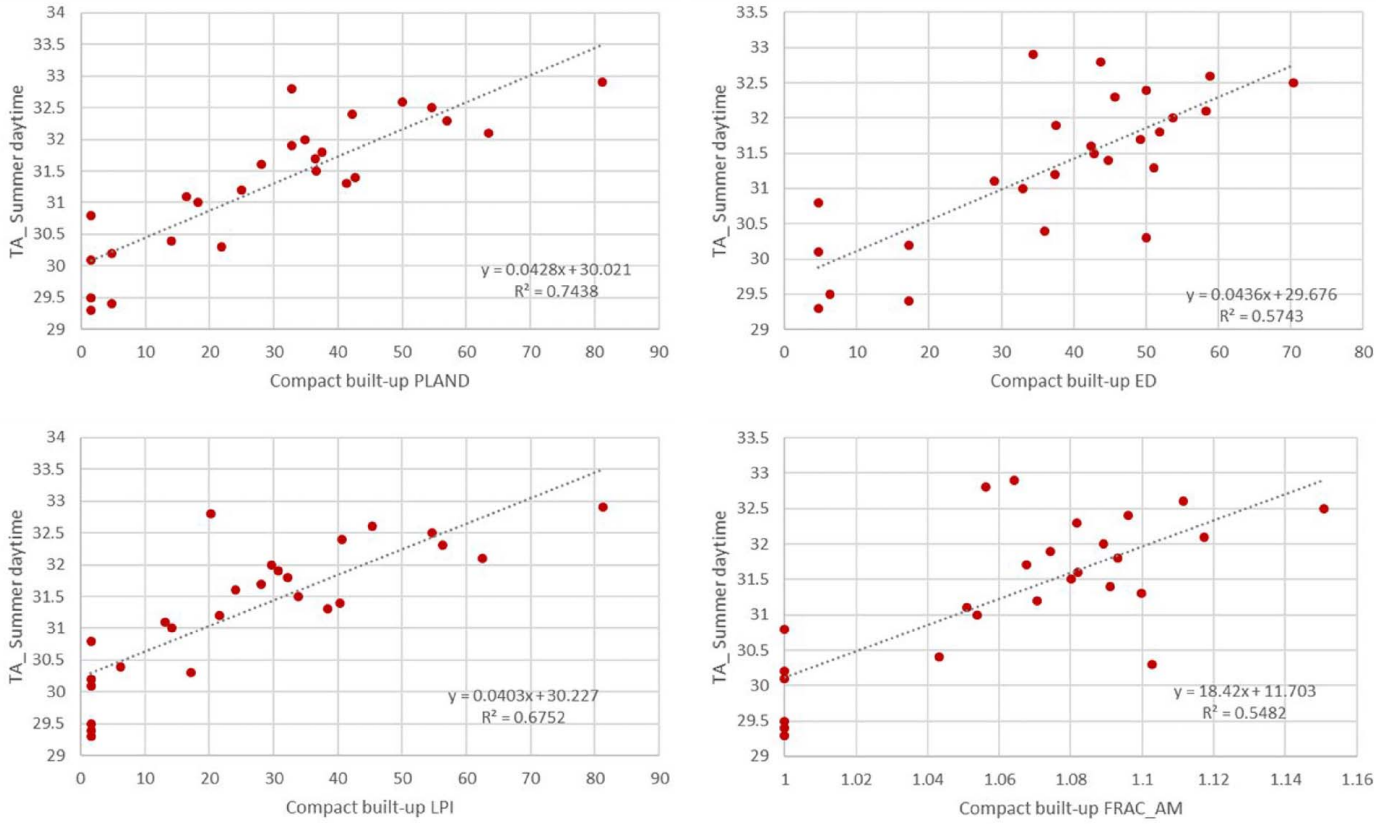

Fig. 10. Correlation distribution of types and temperatures in densely built areas.

positively linearly correlated with Ta, with high correlation coefficients for the area-related indicators (Fig. 10).

The coefficient of determination (R^2) between Ta and PLAND, LPI, ED, and FRAC_AM was 0.74, 0.68, 0.57, and 0.55, respectively. This result revealed that the greater the total of densely built areas in the city, the higher the connectivity and the higher the contact with other urban types, causing a more significant thermal load. The chart for Ta versus PLAND shows densely built areas in a landscape; an increase of 10% in area percentage was correlated with a temperature increase of approximately 0.5°C.

Influence of Green Spaces on the Thermal Environment

Green spaces in the built environment of Taipei accounted for 0%–40% of a landscape area; compared with the densely built areas, the proportion was approximately half. PLAND, LPI, ED, and FRAC_AM were all negatively correlated with Ta, unlike densely built areas. All correlation coefficients were large (Fig. 11).

The coefficient of determination (R^2) between Ta and PLAND, ED, LPI, and FRAC_AM was 0.52, 0.2, 0.52, and 0.25, respectively. Therefore, the greater the area of green spaces in the city and the higher the connectivity, the greater the contact with other urban types, resulting in a better cooling effect on the area. In the chart of Ta versus PLAND, a 10% increase in green spaces was correlated with the approximately 0.3°C cooling effects. The range of confidence for the area ratio was within 40%.

Class-Level Distribution Characteristics and Air Temperature

The densely built areas and green areas were the two largest areas in Taipei's built environment, and their impacts on the thermal environment were the opposite. The Ta characteristics caused by the distribution of densely built areas and green areas were crucial. Dense buildings were positively correlated with temperature, whereas green areas were negatively correlated with temperature overall.

For both densely built and green areas, the area-related indicators had strong correlations with Ta; however, the shape-related indicators also had a certain influence. If two landscapes had the same area, their form was the main reason for temperature effects. Urban morphology had a strong influence on summer daytime temperature.

The class-level correlation analysis revealed that the larger the area of densely built areas in the city and the higher the connectivity with a more significant interface with other urban types resulted in a higher thermal load on the area. In contrast, green spaces resulted in the opposite thermal effect. Green belts must be connected but scattered throughout the landscape. The contact between green spaces can have a continuous cooling effect on the city. If green spaces are too concentrated in one area, the cooling effect is limited to that area and cannot spread outward.

Application to Urban Planning Recommendations

Due to the topographical characteristics of the Taipei basin, natural ventilation is constrained in the city. In addition to being highly developed and having a dense population, the city has poor overall thermal comfort. Therefore, this study performed LEM analysis to identify different landscape types and used the features to summarize the optimal types for future urban planning (Fig. 12).

Taking the scale of the landscape grid in this study as an example, when densely built areas and green belts occupy one-quarter of the area of a landscape grid square, this study recommends that the schematic presented in Fig. 13 can be used for conceptual design

Downloaded from ascelibrary.org by Kuo An Hung on 02/28/24. Copyright ASCE. For personal use only; all rights reserved.

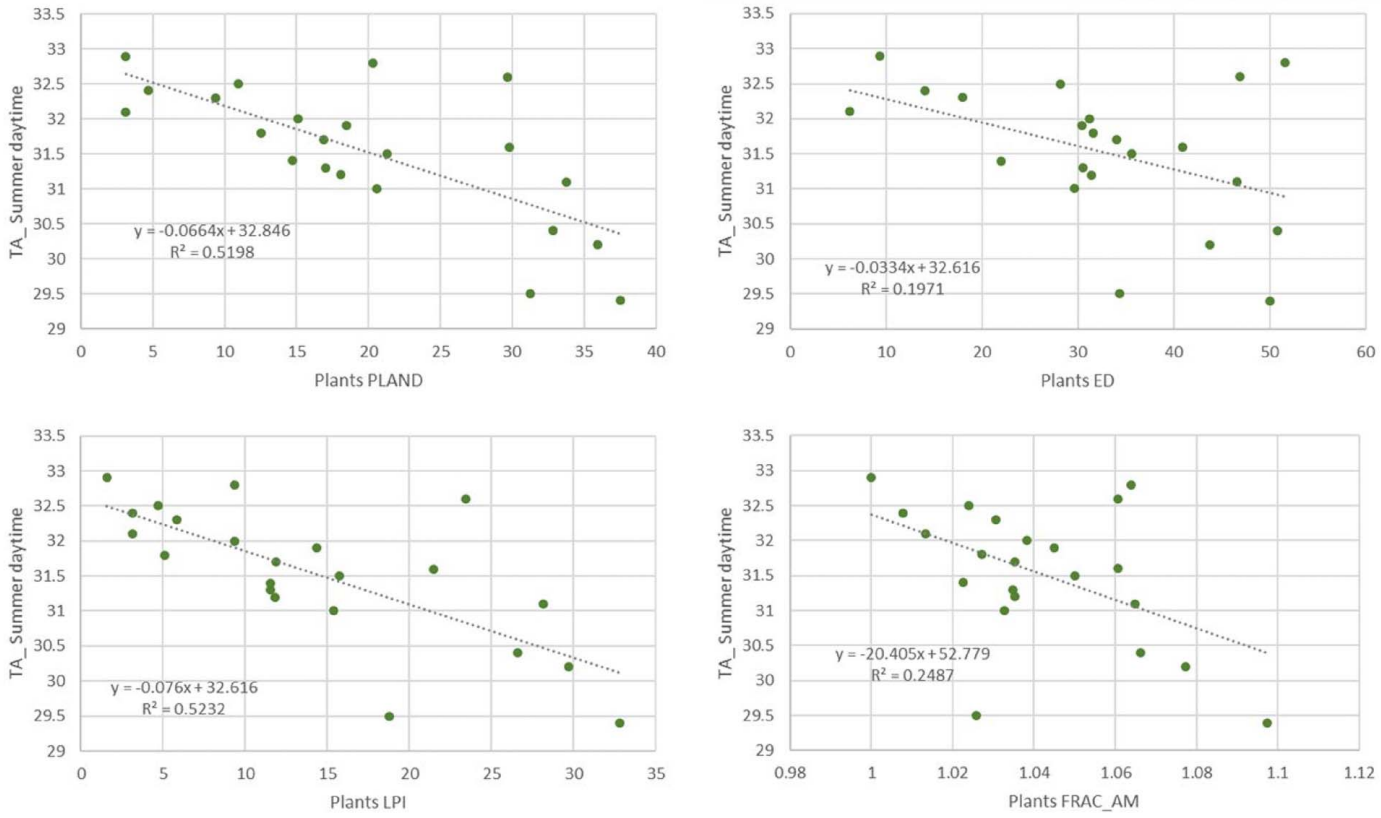

Fig. 11. Correlation distribution of types and temperatures in green areas.

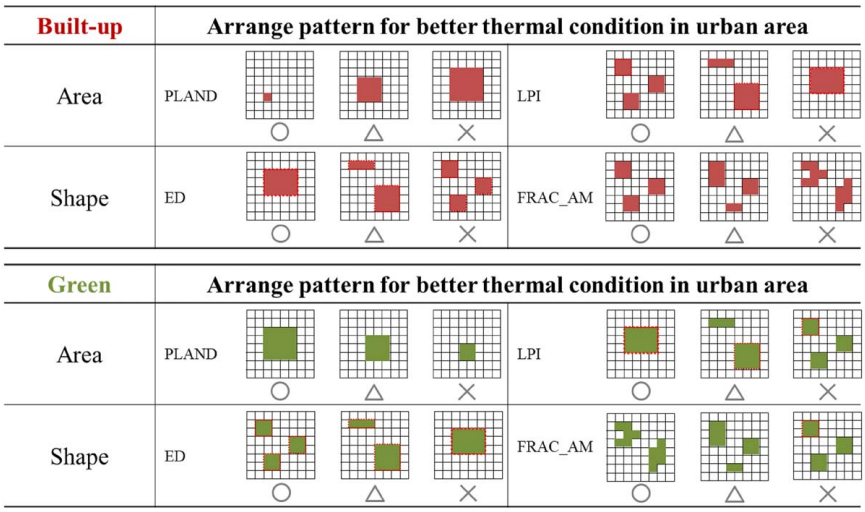

Fig. 12. Arrangement of the pattern of thermal conditions for built-up and green areas.

planning. For dense construction areas, buildings should be constructed in uniform blocks (rectangles or squares), external contact boundaries should be minimized, and the optimal result should be obtained using a single large block. For green belt areas, contact should be high (suitable organic shapes), and green belts should be linked to create corridors or be placed similarly to a checkerboard to promote cooling.

In addition to changing the style of development, increasing the proportions of open building environments and reducing the number of overly dense building areas can create green corridors and slow the accumulation of heat while maintaining the city's development intensity.

Discussion

Improvement in the Definition and Data Acquisition of the Urban Built Environment

Previously, many studies on the urban built environment and thermal environments have utilized the area proportion of different land uses, such as residential, commercial, and industrial areas, as a factor, and the area of land cover, such as buildings, green spaces, and water bodies in the analysis of explain the relationship between surface features and temperature (Eliasson and Svensson 2003; Feddema et al. 2005; Buyadi et al. 2013; Deng et al. 2013; Chen

Downloaded from ascelibrary.org by Kuo An Hung on 02/28/24. Copyright ASCE. For personal use only; all rights reserved.

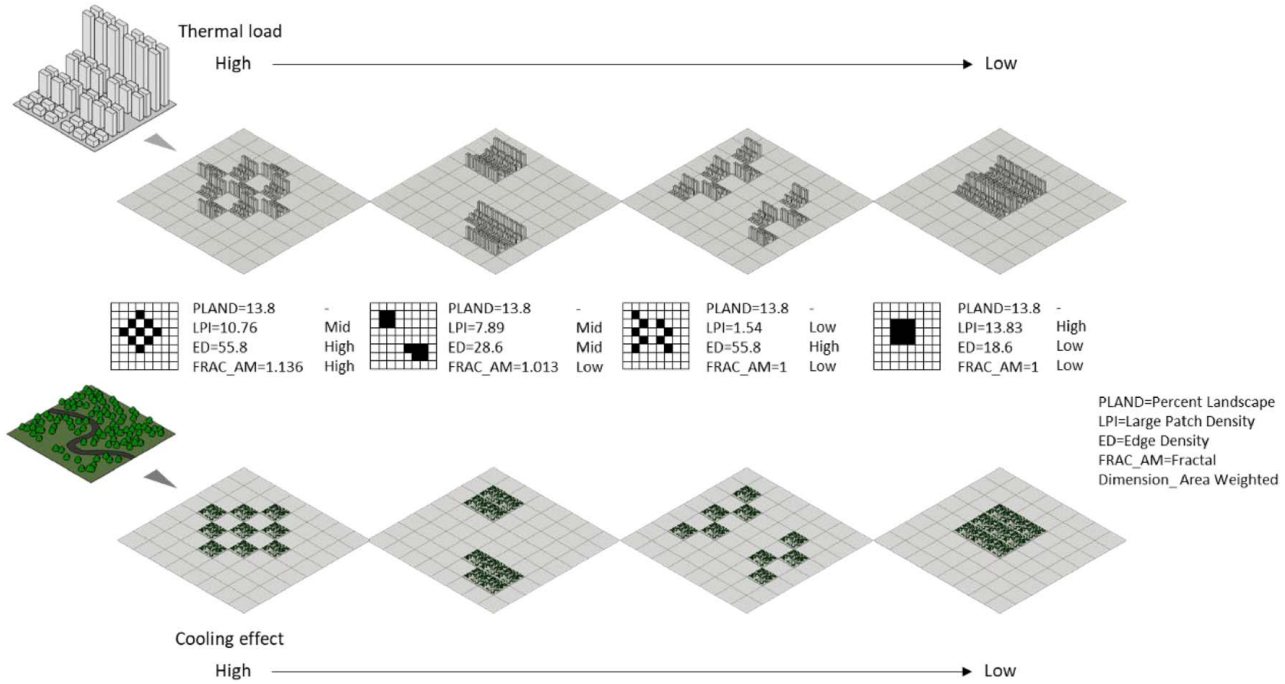

Fig. 13. Distribution of the influence of densely built areas and green space on temperature.

et al. 2017, 2018; Lu et al. 2021). However, these approaches have been effective in some cities because the built environment becomes more and more complex under urbanization, including mixed land use and the formation of diverse buildings and neighborhoods of different heights and densities.

The past conception of the urban built environment has to be reconsidered and redefined, and the methodology of using area ratio to investigate the impacts of the thermal environment has to explore the impacts due to the distribution pattern and morphological characteristics at a more profound scale. Therefore, by combining the two systems of the LCZ and LEM in this study, it is possible to suggest that, for the same area of land, the centralization of residential areas will have the potential to reduce the overall average temperature of the city, and for the same area of land, the green space should be distributed more sporadically in each area of the city to reduce the average temperature of the whole city, and so on. This is a conclusion that could not be reached by using area ratio alone in the past, and it is also an effective way to provide more diversified and sustainable suggestions for urban development and urban planning.

The advantage of this study is also in the accessibility of urban built environment information. Previously, detailed layers were needed to quantify the built environment information in a region, which was often time-consuming and had to be purchased, whereas in this study, the urban pattern training and classification can be done quickly and free of charge through satellite information, which greatly saves the cost of funds and time, and the data can be updated instantly in different time intervals so that it can be applied to different periods in the different research areas.

Application Restrictions

Data have not usually been easy to obtain, and this study used a combination of the LCZ and LEM to develop a method suitable for determining urban development and distribution characteristics to discuss their impact on the thermal environment.

However, the LCZ classification system is limited by differences in the subjective cognition of system's trainers. Even if definitions exist for environmental parameters, the supervised classification and selection of areas will still differ due to users' cognitive differences, potentially resulting in classification errors.

Also, in research and analysis, the LEM is affected by the classification of surface types. Therefore, the local built environment's characteristics must be considered when using the analysis method employed in this study. Not all areas will have the same result.

Therefore, although the LEM can quantify the urban built environment and determine the effects of different arrangements and environments on the urban environment, in subsequent analysis, research can go beyond classification type to select areas using more urban morphology detail.

In the analysis process, the analysis items corresponding to different indicators must be tested individually, and the significance of various indicators must be explored. The analysis results should be verified using actual scenarios to prove the impact of urban structures.

Conclusions

This study employs urban structures to understand the relationship of these structures with the urban thermal environment and establishes a basis for urban planning improvement based on the differences in urban land types.

To quantify differences in urban structure and type, this study employs urban form as the leading environmental observation factor and LCZs, which combine land morphology with three-dimensional classification, to classify urban forms at 100-m resolution. The LCZs are originally classified into 17 types, which this study streamlined into 5 types according to land pattern and land use. The classification results are then used as the basic unit patch for calculating the following four LEM class-level indicators at 800-m resolution: the area-related indicators PLAND and LPI and the shape-related indicators ED and FRAC_AM. These

Downloaded from ascelibrary.org by Kuo An Hung on 02/28/24. Copyright ASCE. For personal use only; all rights reserved.

indicators are used in quantitative analysis of the impact of the urban environment on thermal environments.

The research results reveal that the city's thermal environment was affected by different urban forms and different LCZs produced different air temperature distributions in the hot season. For example, the average temperature in densely built areas is lower than in low-rise buildings and natural areas. The LEM is used to explore the urban pattern and composition methods and reveal that the layout and distribution of dense building areas in the built environment affected the thermal environment's difference. An increase in the four indicators results in a temperature rise. In the relatively green spaces in the urban built environment, the four indicators are negatively correlated with temperature. If the thermal environment is taken into urban planning consideration in the urban built environment, the planning for building areas and green belts should be completely different.

This study suggests that if subsequent urban planners take the urban thermal environment as the foundation, it should be possible to refer to the densely built areas' dense distribution and reduce their contact with the surrounding environment. By contrast, green belts can be highly connected but scattered to improve contact with the surrounding environment, achieving a continuous cooling effect on the city in the hot season.

Data Availability Statement

Some or all data, models, or codes that support the findings of this study are available from the corresponding author upon reasonable request.

Acknowledgments

This study was organized and is summarized as part of the master's thesis of Tzu-Wen Lo. The authors thank her for her effort in the preliminary investigation and analysis. The authors also thank the Ministry of Science and Technology of Taiwan for financially supporting this research under Contract Nos. 108-2221-E-006-008 -MY3 and 111-2221-E-343-001-MY3.

Author contributions: Yu-Cheng Chen and Tzu-Wen Lo carried out the experiment. Yu-Cheng Chen wrote the manuscript with support from Kuo-An Hung. Wan-Yu Shih and Tzu-Ping Lin helped supervise the project. All authors reviewed the manuscript.

References

Alifu, H., Y. Hirabayashi, Y. Imada, and H. Shiogama. 2022. "Enhancement of river flooding due to global warming." *Sci. Rep.* 12: 20687. https://doi.org/10.1038/s41598-022-25182-6.

Arsad, F. S., R. Hod, N. Ahmad, R. Ismail, N. Mohamed, M. Baharom, Y. Osman, M. F. M. Radi, and F. Tangang. 2022. "The impact of heatwaves on mortality and morbidity and the associated vulnerability factors: A systematic review." *Int. J. Environ. Res. Public Health* 19 (23): 16356. https://doi.org/10.3390/ijerph192316356.

Baker, L. A., A. J. Brazel, N. Selover, C. Martin, N. McIntyre, F. R. Steiner, A. Nelson, and L. Musacchio. 2002. "Urbanization and warming of Phoenix (Arizona, USA): Impacts, feedbacks and mitigation." *Urban Ecosyst.* 6: 183–203. https://doi.org/10.1023/A:1026101528700.

Bechtel, B., P. Alexander, J. Böhner, J. Ching, O. Conrad, J. Feddema, M. Gerald, L. See, and I. Stewart. 2015. "Mapping local climate zones for a worldwide database of the form and function of cities." *ISPRS Int. J. Geo-Inf.* 4 (1): 199–219. https://doi.org/10.3390/ijgi4010199.

Beck, C., A. Straub, S. Breitner, J. Cyrys, A. Philipp, J. Rathmann, A. Schneider, K. Wolf, and J. Jacobeit. 2018. "Air temperature characteristics of local climate zones in the Augsburg urban area (Bavaria, southern Germany) under varying synoptic conditions." *Urban Clim.* 25: 152–166. https://doi.org/10.1016/j.uclim.2018.04.007.

Becker, R., C. Schüth, R. Merz, T. Khaliq, M. Usman, T. Beek, R. Kumar, and S. Schulz. 2023. "Increased heat stress reduces future yields of three major crops in Pakistan's Punjab region despite intensification of irrigation." *Agric. Water Manage.* 281: 108243. https://doi.org/10.1016/j.agwat.2023.108243.

Buyadi, S. N. A., W. M. N. Wan Mohd, and A. Misni. 2013. "Impact of land use changes on the surface temperature distribution of area surrounding the National Botanic Garden, Shah Alam." *Procedia Social Behav. Sci.* 101: 516–525. https://doi.org/10.1016/j.sbspro.2013.07.225.

Cai, M., C. Ren, Y. Xu, W. Dai, and X. M. Wang. 2016. "Local climate zone study for sustainable megacities development by using improved WUDAPT methodology—A case study in Guangzhou." *Procedia Environ. Sci.* 36: 82–89. https://doi.org/10.1016/j.proenv.2016.09.017.

Campbell, S., T. A. Remenyi, C. J. White, and F. H. Johnston. 2018. "Heatwave and health impact research: A global review." *Health Place* 53: 210–218. https://doi.org/10.1016/j.healthplace.2018.08.017.

Chen, Y., J. Wu, K. Yu, and D. Wang. 2020. "Evaluating the impact of the building density and height on the block surface temperature." *Build. Environ.* 168: 106493. https://doi.org/10.1016/j.buildenv.2019.106493.

Chen, Y.-C., Y.-J. Liao, C.-K. Yao, T. Honjo, C.-K. Wang, and T.-P. Lin. 2019a. "The application of a high-density street-level air temperature observation network (HiSAN): The relationship between air temperature, urban development, and geographic features." *Sci. Total Environ.* 685: 710–722. https://doi.org/10.1016/j.scitotenv.2019.06.066.

Chen, Y.-C., T.-P. Lin, and C.-T. Lin. 2017. "A simple approach for the development of urban climatic maps based on the urban characteristics in Tainan, Taiwan." *Int. J. Biometeorol.* 61 (6): 1029–1041. https://doi.org/10.1007/s00484-016-1282-0.

Chen, Y.-C., T.-W. Lo, W.-Y. Shih, and T.-P. Lin. 2019b. "Interpreting air temperature generated from urban climatic map by urban morphology in Taipei." *Theor. Appl. Climatol.* 137 (3–4): 2657–2662. https://doi.org/10.1007/s00704-018-02764-x.

Chen, Y.-C., C.-K. Yao, T. Honjo, and T.-P. Lin. 2018. "The application of a high-density street-level air temperature observation network (HiSAN): Dynamic variation characteristics of urban heat island in Tainan, Taiwan." *Sci. Total Environ.* 626: 555–566. https://doi.org/10.1016/j.scitotenv.2018.01.059.

CWBT (Central Weather Bureau of Taiwan). 2011. "Monthly report on climate system." Accessed May 29, 2018. http://www.cwb.gov.tw/V7/forecast/long/long_season.htm.

Deng, X. Z., C. H. Zhao, and H. M. Yan. 2013. "Systematic modeling of impacts of land use and land cover changes on regional climate: A review." *Adv. Meteorol.* 2013: 317678.

Department of Civil Affairs, Taipei City Government. 2017. "2017-Statistics in population and each district households." Accessed March 15, 2018. https://ca.gov.taipei/News_Content.aspx?n=8693DC9620A1AABF&sms=D19E9582624D83CB&s=EE7D5719108F4026.

Department of Civil Affairs, Taipei City Government. 2022. "2022-Statistics in population and each district households." Accessed January 20, 2023. https://reurl.cc/ZWdm4g.

Dong, J., J. Peng, X. He, J. Corcoran, S. Qiu, and X. Wang. 2020. "Heatwave-induced human health risk assessment in megacities based on heat stress-social vulnerability-human exposure framework." *Landscape Urban Plann.* 203: 103907. https://doi.org/10.1016/j.landurbplan.2020.103907.

Ebi, K. L., et al. 2021. "Extreme weather and climate change: Population health and health system implications." *Annu. Rev. Public Health* 42: 293–315. https://doi.org/10.1146/annurev-publhealth-012420-105026.

Downloaded from ascelibrary.org by Kuo An Hung on 02/28/24. Copyright ASCE. For personal use only; all rights reserved.

Eliasson, I., and M. K. Svensson. 2003. "Spatial air temperature variations and urban land use—A statistical approach." *Meteorol. Appl.* 10 (2): 135–149. https://doi.org/10.1017/S1350482703002056.

Feddema, J. J., K. W. Oleson, G. B. Bonan, L. O. Mearns, L. E. Buja, G. A. Meehl, and W. M. Washington. 2005. "The importance of land-cover change in simulating future climates." *Science* 310: 1674–1678. https://doi.org/10.1126/science.1118160.

Figueiredo, R., and M. Martina. 2016. "Using open building data in the development of exposure data sets for catastrophe risk modelling." *Nat. Hazards Earth Syst. Sci.* 16: 417–429. https://doi.org/10.5194/nhess-16-417-2016.

Forman, R. T. T. 1995. *Land mosaics: The ecology of landscapes and regions*. Cambridge, UK: Cambridge University Press.

Frank, S., C. Fürst, L. Koschke, and F. Makeschin. 2012. "A contribution towards a transfer of the ecosystem service concept to landscape planning using landscape metrics." *Ecol. Indic.* 21: 30–38. https://doi.org/10.1016/j.ecolind.2011.04.027.

Giridharan, R., and R. Emmanuel. 2018. "The impact of urban compactness, comfort strategies and energy consumption on tropical urban heat island intensity: A review." *Sustainable Cities Soc.* 40: 677–687. https://doi.org/10.1016/j.scs.2018.01.024.

Gu, L., J. Chen, J. Yin, L. J. Slater, H.-M. Wang, Q. Guo, M. Feng, H. Qin, and T. Zhao. 2022. "Global increases in compound flood—Hot extreme hazards under climate warming." *Geophys. Res. Lett.* 49: e2022GL097726. https://doi.org/10.1029/2022GL097726.

Harp, R. D., and K. B. Karnauskas. 2020. "Global warming to increase violent crime in the United States" *Environ. Res. Lett*. 15: 034039. https://doi.org/10.1088/1748-9326/ab6b37.

Heshmat Mohajer, H. R. H., L. Ding, and M. Santamouris. 2022. "Developing heat mitigation strategies in the urban environment of Sydney, Australia." *Buildings* 12 (7): 903. https://doi.org/10.3390/buildings12070903.

Honjo, T., H. Yamato, T. Mikami, and C. S. B. Grimmond. 2015. "Network optimization for enhanced resilience of urban heat island measurements." *Sustainable Cities Soc.* 19: 319–330. https://doi.org/10.1016/j.scs.2015.02.004.

Hu, Y., and G. Jia. 2010. "Influence of land use change on urban heat island derived from multi-sensor data." *Int. J. Climatol.* 30 (9): 1382–1395. https://doi.org/10.1002/joc.1984.

Hung, K.-A., Y.-W. Hsu, Y.-C. Chen, and T.-P. Lin. 2023. "Influence of microclimate control on the growth of asparagus under greenhouse in tropical climates." *Int. J. Biometeorol.* 67: 1225–1235. https://doi.org/10.1007/s00484-023-02490-8.

Jia, S., and Y. Wang. 2021. "Effect of heat mitigation strategies on thermal environment, thermal comfort, and walkability: A case study in Hong Kong." *Build. Environ.* 201: 107988. https://doi.org/10.1016/j.buildenv.2021.107988.

Kaloustian, N., and B. Bechtel. 2016. "Local climatic zoning and urban Heat Island in Beirut." *Procedia Eng.* 169: 216–223. https://doi.org/10.1016/j.proeng.2016.10.026.

Kim, J.-I., M.-J. Jun, C.-H. Yeo, K.-H. Kwon, and J. Y. Hyun. 2019. "The effects of land use zoning and densification on changes in land surface temperature in Seoul." *Sustainability* 11: 7056. https://doi.org/10.3390/su11247056.

Kong, F., H. Yin, P. James, L. R. Hutyra, and H. S. He. 2014. "Effects of spatial pattern of greenspace on urban cooling in a large metropolitan area of eastern China." *Landscape Urban Plann.* 128: 35–47. https://doi.org/10.1016/j.landurbplan.2014.04.018.

Kotharkar, R., and M. Surawar. 2016. "Land use, land cover, and population density impact on the formation of canopy urban heat islands through traverse survey in the Nagpur urban area, India." *J. Urban Plann. Dev.* 142 (1): 04015003. https://doi.org/10.1061/(ASCE)UP.1943-5444.0000277.

Kovats, R. S., and S. Hajat. 2008. "Heat stress and public health: A critical review." *Annu. Rev. Public Health* 29: 41–55. https://doi.org/10.1146/annurev.publhealth.29.020907.090843.

Leitão, A. B., and J. Ahern. 2002. "Applying landscape ecological concepts and metrics in sustainable landscape planning." *Landscape Urban Plann.* 59: 65–93. https://doi.org/10.1016/S0169-2046(02)00005-1.

Lin, T.-P., Y.-C. Chen, and A. Matzarakis. 2017. "Urban thermal stress climatic mapping: Combination of long-term climate data and thermal stress risk evaluation." *Sustainable Cities Soc.* 34: 12–21. https://doi.org/10.1016/j.scs.2017.05.022.

Lu, Y., W. Yue, and Y. Huang. 2021. "Effects of land Use on land surface temperature: A case study of Wuhan, China." *Int. J. Environ. Res. Public Health* 18 (19): 9987. https://doi.org/10.3390/ijerph18199987.

McGarigal, K., and B. J. Marks. 1995. *FRAGSTATS: Spatial pattern analysis program for quantifying landscape structure*. Corvallis, OR: USDA, Forest Service, Pacific Northwest Research Station.

Naveh, Z., and S. Lieberman. 1985. *Landscape ecology: Theory and application*. New York: Springer.

Oke, T. R. 1973. "City size and the urban heat island." *Atmos. Environ.* 7: 769–779. https://doi.org/10.1016/0004-6981(73)90140-6.

Oke, T. R. 1988. "Street design and urban canopy layer climate." *Energy Build.* 11 (1–3): 103–113. https://doi.org/10.1016/0378-7788(88)90026-6.

Oraskari, J., and S. Törmä. 2017. "Access control for Web of building data: Challenges and directions." In *Ework and EBusiness in architecture, engineering and construction*, edited by S. Christodoulou and R. Scherer, 45–53. Boca Raton, FL: CRC Press.

Qin, S., Y. Liu, G. Yu, and R. Li. 2023. "Assessing the potential of integrated shading devices to mitigate overheating risk in university buildings in severe cold regions of China: A case study in Harbin." *Energies* 16 (17): 6259. https://doi.org/10.3390/en16176259.

Ren, C., K. L. Lau, K. P. Yiu, and E. Ng. 2013. "The application of urban climatic mapping to the urban planning of high-density cities: The case of Kaohsiung, Taiwan." *Cities* 31: 1–16. https://doi.org/10.1016/j.cities.2012.12.005.

Schiermeier, Q. 2011. "Increased flood risk linked to global warming." *Nature* 470: 316. https://doi.org/10.1038/470316a.

Shih, W. 2017. "Greenspace patterns and the mitigation of land surface temperature in Taipei metropolis." *Habitat Int.* 60: 69–80. https://doi.org/10.1016/j.habitatint.2016.12.006.

Stewart, I. D., and T. R. Oke. 2012. "Local climate zones for urban temperature studies." *Bull. Am. Meteorol. Soc.* 93 (12): 1879–1900. https://doi.org/10.1175/BAMS-D-11-00019.1.

Stewart, I. D., T. R. Oke, and E. S. Krayenhoff. 2014. "Evaluation of the 'local climate zone' scheme using temperature observations and model simulations." *Int. J. Climatol.* 34 (4): 1062–1080. https://doi.org/10.1002/joc.3746.

Su, W., C. Gu, and G. Yang. 2010. "Assessing the impact of land use/land cover on urban heat island pattern in Nanjing City, China." *J. Urban Plann. Dev.* 136 (4): 365–372. https://doi.org/10.1061/(ASCE)UP.1943-5444.0000033.

Syrbe, R.-U., and U. Walz. 2012. "Spatial indicators for the assessment of ecosystem services: Providing, benefiting and connecting areas and landscape metrics." *Ecol. Indic.* 21: 80–88. https://doi.org/10.1016/j.ecolind.2012.02.013.

Tabari, H. 2020. "Climate change impact on flood and extreme precipitation increases with water availability." *Sci. Rep.* 10: 13768. https://doi.org/10.1038/s41598-020-70816-2.

Teo, Y. H., M. A. B. H. Makani, W. Wang, L. Liu, J. H. Yap, and K. H. Cheong. 2022. "Urban heat island mitigation: GIS-based analysis for a tropical city Singapore." *Int. J. Environ. Res. Public Health* 19 (19): 11917. https://doi.org/10.3390/ijerph191911917.

Tiihonen, J., P. Halonen, L. Tiihonen, H. Kautiainen, M. Storvik, and J. Callaway. 2017. "The association of ambient temperature and violent crime." *Sci. Rep.* 7 (1): 6543. https://doi.org/10.1038/s41598-017-06720-z.

Turner, M. G. 1989. "Landscape ecology: The effect of pattern on process." *Annu. Rev. Ecol. Syst.* 20: 171–197. https://doi.org/10.1146/annurev.es.20.110189.001131.

Turner, M. G., R. H. Gardner, and R. V. O'Neill. 2001. *Landscape ecology in theory and practice: Pattern and process*. New York: Springer.

Uuemaa, E., M. Antrop, J. Roosaare, R. Marja, and Ü Mander. 2009. "Landscape metrics and indices: An overview of their use in landscape research." *Living Rev. Landscape Res.* 3 (1): 1–28. https://doi.org/10.12942/lrlr-2009-1.

Downloaded from ascelibrary.org by Kuo An Hung on 02/28/24. Copyright ASCE. For personal use only; all rights reserved.

Uuemaa, E., Ü Mander, and R. Marja. 2013. "Trends in the use of landscape spatial metrics as landscape indicators: A review." *Ecol. Indic.* 28: 100–106. https://doi.org/10.1016/j.ecolind.2012.07.018.

Wei, R., D. Song, N. H. Wong, and M. Martin. 2016. "Impact of urban morphology parameters on microclimate." *Procedia Eng.* 169: 142–149. https://doi.org/10.1016/j.proeng.2016.10.017.

Wu, J. 2000. *Landscape ecology: Pattern, process, scale and hierarchy*. Beijing: Higher Education Press.

Yahia, M. W., and E. Johansson. 2014. "Landscape interventions in improving thermal comfort in the hot dry city of Damascus, Syria—The example of residential spaces with detached buildings." *Landscape Urban Plann.* 125: 1–16. https://doi.org/10.1016/j.landurbplan.2014.01.014.

Yang, J., B. Shi, G. Xia, Q. Xue, and S.-J. Cao. 2020. "Impacts of urban form on thermal environment near the surface region at pedestrian height: A case study based on high-density built-up areas of Nanjing City in China." *Sustainability* 12: 1737. https://doi.org/10.3390/su12051737.

Yang, Y., X. Zhang, X. Lu, J. Hu, X. Pan, Q. Zhu, and W. Su. 2018. "Effects of building design elements on residential thermal environment." *Sustainability* 10 (1): 57. https://doi.org/10.3390/su10010057.

Zhang, Y., A. T. Murray, and B. L. Turner. 2017. "Optimizing green space locations to reduce daytime and nighttime urban heat island effects in Phoenix, Arizona." *Landscape Urban Plann.* 165: 162–171. https://doi.org/10.1016/j.landurbplan.2017.04.009.

Zhang, Z., F. van Coillie, E. M. De Clercq, X. Ou, and R. De Wulf. 2013. "Mountain vegetation change quantification using surface landscape metrics in Lancang Watershed, China." *Ecol. Indic.* 31: 49–58. https://doi.org/10.1016/j.ecolind.2012.11.013.

Zhao, C., et al. 2017. "Temperature increase reduces global yields of major crops in four independent estimates." *Proc. Natl. Acad. Sci. USA* 114 (35): 9326–9331. https://doi.org/10.1073/pnas.1701762114.

Zhou, B., D. Rybski, and J. P. Kropp. 2017. "The role of city size and urban form in the surface urban heat island." *Sci. Rep.* 7: 4791. https://doi.org/10.1038/s41598-017-04242-2.

Downloaded from ascelibrary.org by Kuo An Hung on 02/28/24. Copyright ASCE. For personal use only; all rights reserved.